THE MALTA CISTERN MAPPING PROJECT: EXPEDITION II

C. M. Clark
Computer Science Dept.
Cal. Polytechnic State U.
San Luis Obispo, USA
cmclark@calpoly.edu

D. Hiranandani, C. White, M. Boardman, M. Schlachtman, P. Phillips, J. Kuehn
Computer Engineering.
Cal. Polytechnic State U.
San Luis Obispo, USA

T. Gambin
AURORA Special Purpose Trust. Malta
tgambin@hotmail.com

K. Buhagiar
Dept. of Classics and Archeology
University of Malta
keithbuhagiar@onvol.net

ABSTRACT

This paper documents the second of two archeological expeditions that employed several underwater robot mapping and localization techniques. The goal of this project is to explore and map ancient cisterns located on the islands of Malta and Gozo. Dating back to 300 B.C., the cisterns of interest acted as water storage systems for fortresses, private homes, and churches. They often consisted of several connected chambers, still containing water. A Remotely Operated Vehicle (ROV), was deployed into cisterns to obtain video and sonar images. Using a variety of sonar based mapping techniques, two-dimensional maps of 18 different cisterns were created.

I. INTRODUCTION

In February of 2008, the first cistern mapping expedition took place and was successful in creating the first ever 2D maps of Malta's ancient cisterns. In March of 2009, the second mapping expedition took place. Using a new smart tether, a micro-manipulator, and improved control algorithms, investigators worked to generate maps of cisterns never before explored. This paper documents results from the second expedition, and demonstrates improvements on results from the first expedition.

Researchers traveled to 18 archeological sites across the islands of Malta and Gozo. At each site, a search for cistern access points was conducted. Once found, investigators lowered a VideoRay Pro III Remotely Operated Vehicle (ROV) down the access points until the ROV was submerged in the cistern water. The ROV was then tele-operated to navigate the tunnels.

Figure 1: The VideoRay Pro III ROV. In this image, the supporting feet of the ROV have been removed to allow entry through the smallest cistern passage. The cistern was located in a private home of the Mdina fortress.

The VideoRay Pro III, shown in Fig. 1, is a micro ROV class of vehicle with a length of 0.305m. It has two horizontal thrusters located on each side of the main hull to enable differential thrust. A single vertical thruster is located inside the yellow float block. The Pro III comes equipped with compass, depth sensor, front facing color video camera, and rear facing B/W video camera. To obtain sonar measurements, a Tritech SeaSprite scanning sonar was attached to the top of the ROV. To facilitate computer control and mapping, the standard VideoRay system comes with a serial port that permits a PC to receive all sensor data and send thruster control signals. Fig. 2 shows a typical setup site.

Section II of this paper provides a brief background on related mapping systems. Section III gives explanations of the mapping techniques employed. In section IV, results are presented and discussed. Conclusions are drawn in Section V along with future goals.

II. Background

Several methods exist for mapping underwater environments when using underwater robots. The maps constructed are used both for the application at hand (e.g. oceanography, marine biology, archaeology, etc.) and to improve the navigation capabilities of the robot itself.

When a robot is localized with respect to some inertial coordinate frame (i.e. the robot's position is known), mapping while in motion is a much simpler task. An approach typically used when operating wheeled robots within indoor environments is to use an occupancy grid map that is updated via the log likelihood approach that assigns a probability of occupation for that each cell in the grid [1].

A common method used for mapping underwater seafloors involves creating mosaics of bottom images. Once combined, the resulting mosaic can be used as a map with which the robot can localize itself. Such systems do not rely on the deployment of infrastructure like acoustic positioning systems and do not suffer from drift like IMU based systems. For example, in [2] an ROV was equipped with a real-time mosaicking system. In [3], video mosaics were used for Autonomous Underwater Vehicle navigation.

In recent years, a large amount of research has been conducted in the area of Simultaneous Localization and Mapping (SLAM). SLAM techniques have been developed and modified for a large number of applications and environments. A good survey of the core techniques including both Kalman Filtering and Particle Filtering based techniques can be found in [4].

One example of robots conducting SLAM in tunnel systems is found in [5]. In that work, the mapping of underground mines was conducted using an autonomous wheeled robot called "Groundhog". Other relevant work includes the work conducted in underwater robot SLAM. One of the first instances includes the work done in [6], where sonar scans were used to map and track features of the environment. More recently, successful 3D tunnel mapping in underwater environments was demonstrated in [7].

Figure 2: A typical ROV deployment in which the robot is driven by computer, while video feedback is recorded and maps are constructed with sonar data. Note the yellow tether descending into the mouth of the access point. The photo was taken in the Palazzo Falzon courtyard, Mdina.

Unlike the work in [7], this paper describes applications which only permit the passage of small-scale robot systems (i.e. passage opening diameters on the order of 0.3m). This greatly reduces the vehicle payload. Notably, the ROV in this work was equipped only with a depth sensor, compass, smart tether and sonar. To overcome this limitation in sensing, a dynamic model of the ROV was used for the prediction step of both the SLAM and Particle Filter localization algorithm.

III. Mapping Techniques

While exploring the cisterns, control inputs and all sensor data (i.e. video, compass, depth, smart tether and sonar measurements) were logged and in some cases SLAM was conducted in real time. Three techniques were employed for mapping:

1. Manual Mosaicking of Sonar Images
2. Simultaneous Localization and Mapping (SLAM) using Stationary Sonar Scans
3. SLAM while the ROV is moving

To create mosaics of sonar images, the ROV was landed on the floor of cisterns to enable full 360 degree sonar scans while the vehicle was stationary. Scans were recorded from several locations in each cistern. Given a series of overlapping sonar images, operators would manually drag and drop images together to create maps. Examples of maps created in this manner are provided in Fig. 4 (e) and Fig. 4 (h).

For both stationary and moving SLAM, an occupancy grid FastSLAM algorithm [1] was used which fused measurements from sonar, compass, dynamic model, and smart tether. The occupancy grid representation was used since it doesn't require features to be tracked like many other SLAM algorithms. Most cisterns haven't been visited in over 2000 years, making it difficult to predict if observable features would be present.

FastSLAM is a particle filter based approach to SLAM, in which a collection of M particles denoted as X_t is used to model the belief state. For this case, the k^{th} particle consists of an occupancy grid m_t, the robot's state $x_t^k = [x^k\ y^k\ z^k\ \theta^k\ \dot{x}^k\ \dot{y}^k\ \dot{z}^k\ \dot{\theta}^k\ ]_t$, and a weight w_t^k that represents the likelihood that particle k represents the true state. As shown in Table 1, the t^{th} time step of the algorithm updates all particles as new sensor measurements z_t are observed.

Table 1:The FastSLAM Algorithm

1:	**Alg. FastSLAM_occupancy_grids(**X_{t-1}, u_t, z_t**):**
2:	$X_t' = X_t = 0$
3:	*for* $k = 1$ *to* M *do*
4:	x_t^k = **sample_motion_model(**u_t, x_{t-1}^k**)**
5:	w_t^k = **measurement_model_map(**z_t, u_t, m_{t-1}^k**)**
6:	m_t^k = **updated_occupancy_grid(**z_t, u_t, m_{t-1}^k**)**
7:	$X' = X' + \{ x_t^k, m_t^k, w_t^k \}$
8:	*Endfor*
9:	*for* $k = 1$ *to* M *do*
10:	*draw i with probability* $\sim w_t^i$
11:	*add* $\{ x_t^i, m_t^i \}$ *to* X_t
12:	*Endfor*
13:	*return* X_t

The three key steps to this algorithm are on line numbers 4, 5 and 6. The first step calls **sample_motion_model**, which propagates the previous state x_{t-1}^k of the robot forward in time according to the vehicle dynamic model. Such a model was developed by the author and is described in [8]. A certain degree of randomness is added to this propagation, in accordance with the expected variance from the robot's motion model.

The next step in the algorithm invokes the **measurement_model_map** function, which calculates the weight of the k^{th} particle. Two different techniques were used to update the particle weights.

The first weight update technique was based on sonar measurements. At a high level, the expected sonar measurement is calculated given the robot state x_t, and map m_{t-1}. This expected sonar measurement is compared with the actual measurement z_t. If the two measurements are similar, a high weight is returned, otherwise a low weight is returned. Mathematical details of this sensor model are provided in [9].

For a few cisterns, a second weight update technique was used that incorporates smart tether data. The smart tether, produced by KCF technologies, is a tether fitted with strategically placed sensors that determine the location of the ROV relative to an above water GPS receiver. These measurements were differenced with the position in the particle state x_t^k and passed through a normal Probability Distribution Function (PDF) to determine the probability of getting such a smart tether position measurement if the robot was in the state x_t^k. To note, the PDF requires the variance of the smart tether measurements σ^2_{st}.

The last core function of the algorithm, **updated_occupancy_grid**, updates the map with the new sonar measurements. More details of these steps can be found in [9], where methods and results from the 2008 expedition were presented.

IV. Results

Sonar mosaics and occupancy grids were constructed for all 18 sites visited. Occupancy grids were built with grid cells of size 0.20m x 0.20m. When conducting SLAM while the ROV was in motion, the latency of the sonar required the ROV to move at low velocities, on the order of 0.05m/s. The best results, in terms of minimal variance of wall positions in the grid, were obtained with SLAM using stationary scans.

A wide variety of types of cisterns were mapped during the expedition. Their depth, construction type, size, shape, number of chambers, and date of construction all varied. Images in Fig. 3 and Fig. 4 present the most

notable and representative of the 18 sites mapped. Fig. 3 shows still images taken with the ROV's forward facing camera while the ROV was navigating cisterns. Fig. 4 shows access points and the corresponding cistern maps constructed.

Images in Fig. 4 (a) were obtained by exploring site 15, the courtyard at the top of Fort St. Angelos. Several other cisterns explored had a similar elliptical shape and size.

The cistern located in a private home within the Gozo Citadel (site 18) is shown in Fig. 4 (b). This cistern, believed to be built in Roman times based on the shape, was accessed through a hole in the wall of a staircase.

At the top of the Gozo Citadel (site 20) is an access point that led to a smaller cistern. As shown in Fig. 4 (c), the cistern is cylindrical in shape. Within this cistern, the micro-manipulator was used to obtain old pottery shards, (date unknown at time of publishing).

Site 22 was a cistern found in the courtyard of a Franciscan Monastery in the town of Rabat, Malta. Like several other cisterns, this one had very little water left and the sonar map was built using reflections from bottom debris and rocks.

Shown in Fig. 4 (e) are images from a cistern in a private home in Rabat. This particular cistern was unique in its construction and features. The cistern was rectangular in shape. Interestingly, the cistern roof and walls were lined with a series of four archways. An image of one such ceiling arch is shown in Fig. 3 (a).

One of the most complex cisterns was at site 29, shown in Fig. 4 (f). The access point was found in the side of a wall in a Priory in the fortress city of Mdina. The cistern was comprised of three main chambers, connected by tunnels. An image of a passageway to one such tunnel is shown in Fig. 3 (b). Panning up the front camera on the robot revealed several other access points that were covered sometime in the past. This cistern was the only cistern within which two ROVs were simultaneously deployed. Shown in Fig. 3 (c) is a still image recorded from one ROV observing another.

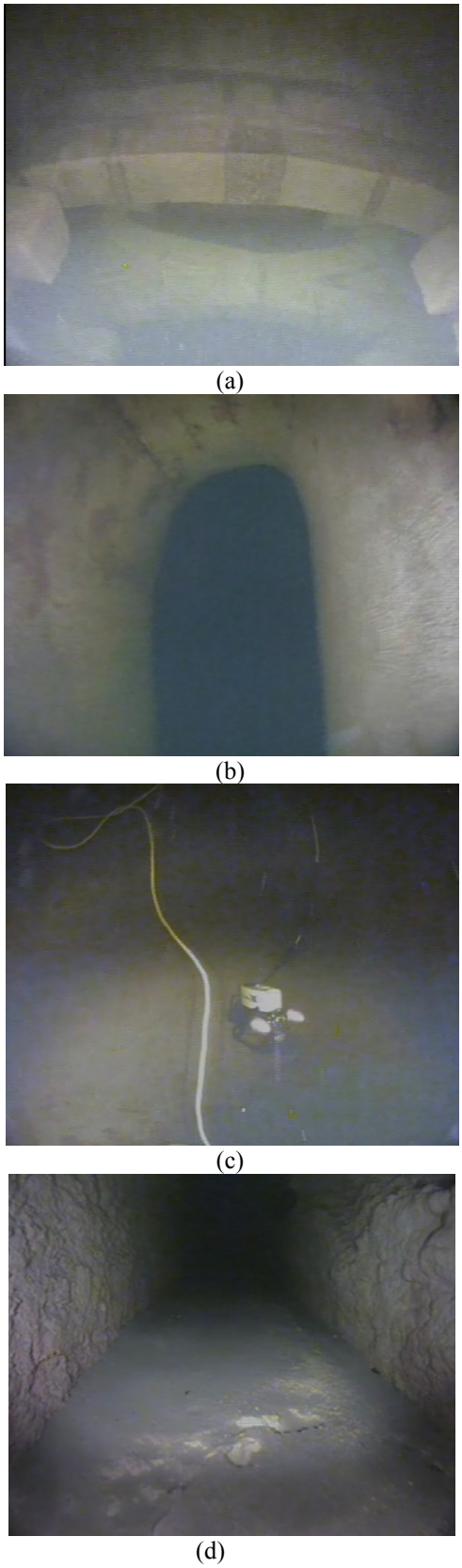

(a) (b) (c) (d)

Figure 3: Images obtained from robot video during deployments in cisterns.

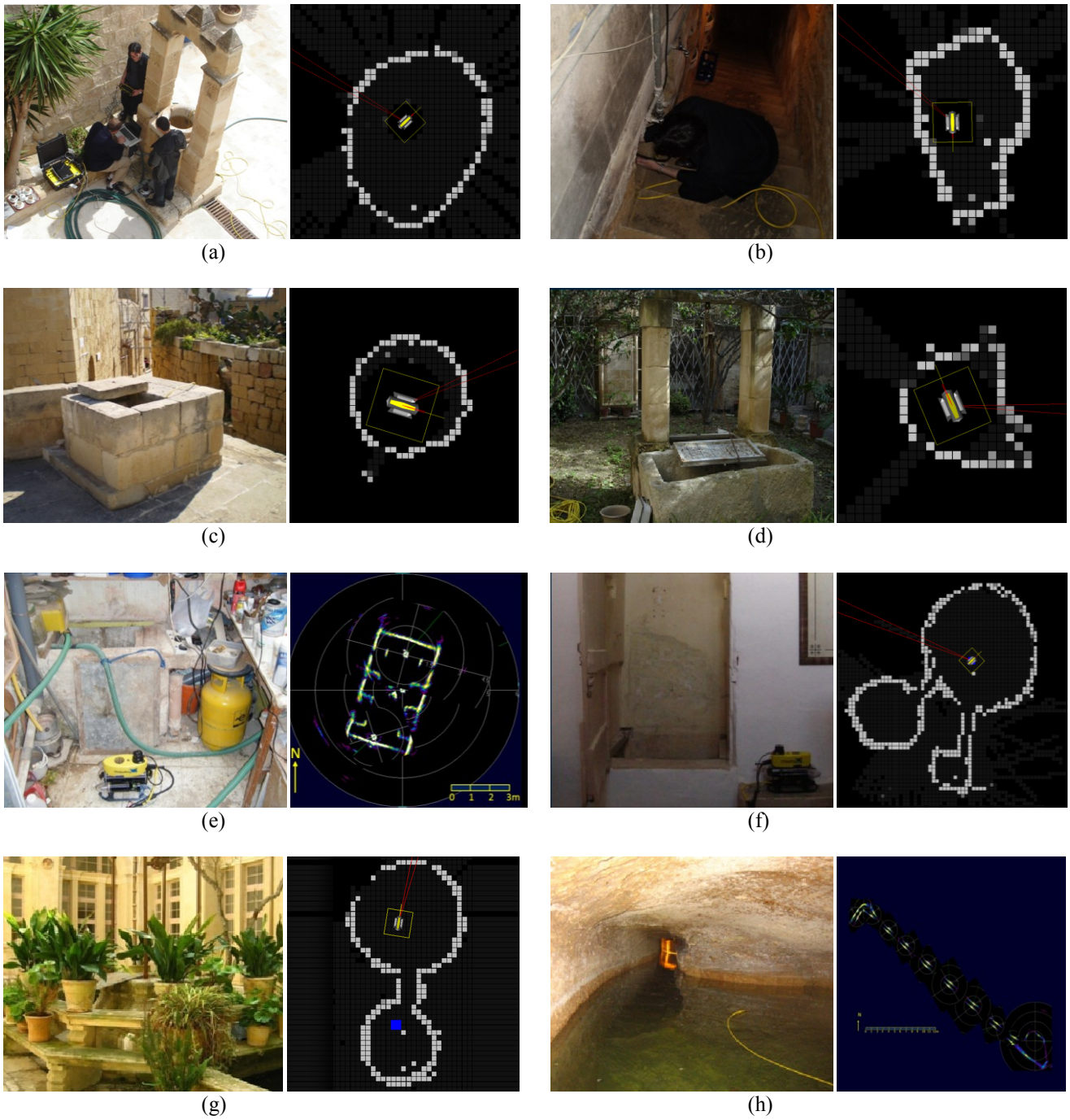

Figure 4: Maps created using for a variety of sites. Access points are shown on left. Occupancy grid maps have cell size of 0.2m x 0.2m. Scales are given on maps created with sonar scan mosaics.

Site 30 was a cistern, found in the courtyard of the same Mdina Priory of site 29. The cistern consists of two separate chambers connected by a narrow passage, (see Fig. 4 g).

Finally, Fig. 4 (h) shows the cistern in site 32. This cistern, or rather a water gallery probably dating to the 12th or 13th century AD, was accessed via a narrow tunnel giving direct access to the water table. During exploration, the ROV travelled down this long tunnel until the end of the tether was reached. Fig. 3 (d) shows a still image of the tunnel from the point of view of the ROV.

V. Conclusions & Future Work

The expedition described in this paper proved successful in constructing maps of 18 different cisterns within 6 days of fieldwork. A variety of techniques were used, but using stationary 360 degree sonar scans within the FastSLAM algorithm produced the occupancy grid maps with minimal variance in wall position.

Future expeditions will include mapping of cisterns in two cities of Italy. Also, it is hoped that methods for 3D mapping will be developed using different configurations of the scanning sonar, or a short range 3D laser scanner. Ideally, new 3D visualizations would be constructed to accompany such 3D maps.

Most importantly, these maps will be integrated into the archeological study that motivates this research, a long term study on the history of Maltese water management systems [10].

References

[1] H.P Moravec, "Sensor fusion in certainty grids for mobile robots," AI Magazine, Vol 9, pp. 61-74, 1988.

[2] K. Richmond and S. M. Rock,, "An operational real-time large-scale visual mosaicking and navigation system," Proceedings of the 2006 MTS/IEEE OCEANS conference, September 2006.

[3] H. Sakai, T. Tanaka, T. Mori, S. Ohata, K. Ishii, and T. Ura, "Underwater video mosaicking using AUV and its application to vehicle navigation," Proceedings of the 2004 International Symposium on Underwater Technology, April 2004.

[4] S. Thrun, W. Burgard and D. Fox, "Probabilistic Robotics," MIT Press, 2005.

[5] C. Baker, A.C. Morris, D. Ferguson, S. Thayer, C. Whittaker, Z. Omohundro, C. Reverte, W.L. Whittaker, D. Haehnel, and S. Thrun,, "A Campaign in Autonomous Mine Mapping," Proceedings of the IEEE Conference on Robotics and Automation (ICRA), April 2004.

[6] S. B. Williams, P. Newman, G. Dissanayake, H. Durrant-Whyte, "Autonomous underwater simultaneous localisation and map building," Proceedings of the 2000 IEEE International Conference, 2000.

[7] N. Fairfield, G. Kantor, and D. Wettergreen, "Real-time SLAM with octree evidence grids for exploration in underwater tunnels," Journal of Field Robotics, Vol 24, Issue 1-2, pp. 03-21, October 2006.

[8] W. Wang, and C. M. Clark, "Modeling and simulation of the VideoRay Pro III underwater vehicle," Proceedings of the IEEE OCEANS'06 Asia Pacific IEEE Conference, May 2006.

[9] Clark, C.M, Olstad, C.S., Buhagiar, K., and Gambin, T., Archaeology via Underwater Robots: Mapping and Localization within Maltese Cistern Systems, Proc. of the 10th International Conference on Control, Automationa, Robotics and Vision (ICARCV'08), Dec, 2008.

[10] Buhagiar, K., 'Water Management Strategies and the Cave-Dwelling phenomenon in Late-medieval Malta', Medieval Archaeology, 51, 2007.